Measurement 42 (2009) 1011–1016

Contents lists available at ScienceDirect

Measurement

journal homepage: www.elsevier.com/locate/measurement

Study of ultra-miniature giant magneto resistance sensor system based on 3D static magnetic analysis technique

T. Lan [a], Y.W. Liu [a], M.H. Jin [a], S.W. Fan [a], Z.P. Chen [a], H. Liu [a,b,*]

[a] State Key Laboratory of Robotics and System (HIT), Harbin, PR China
[b] Institute of Robotics and System Dynamics, German Aerospace Center, Germany

ARTICLE INFO

Article history:
Received 27 November 2008
Accepted 3 March 2009
Available online 12 March 2009

Keywords:
Magnetic sensor
Finite element techniques
3D static magnetic analysis
GMR sensor
MEMS

ABSTRACT

In this study, a method for the modeling of ferromagnetic component of an ultra-miniature giant magneto resistance (GMR) sensor system is presented. The goal of the modeling is to design appropriate angular sensor system for the highly integrated DLR/HIT II 5-finger dexterous robot hand. A 3D static magnetic analysis modeling is used to avoid sensor damage by the excessive magnetic intensity and disorientation when other magnetic fields disturb the primary field. Using the finite element results, appropriate shape and size of ferromagnetic component is compared and optimized. A simplified signal processing circuit is also given for the ultra-miniature GMR sensor system. Finally experimental results show an angular accuracy of less than $\pm 1^{\circ}$ with only the residual offset compensation of ultra-miniature GMR sensor system is obtained. Integration experiences reveal the challenges associated with obtaining the required capabilities within the desired size.

1. Introduction

In general, further system miniaturization will certainly create demands for a continuous down-scaling of sensor functions in a variety of different application fields [1]. When developing sensors for measuring angular signal in miniature systems, it becomes obvious that the basic sensor has many limitations and imperfections (e.g. size, working distance, accuracy and offset) which prevent the designer from achieving the required specifications. To improve the basic sensor performance, one option is to try and refine the sensor itself using better materials, production methods, etc. This choice is generally an expensive one. Another option is to incorporate the sensor into a system which has the unique objective of improving the basic sensor performance. And one important trend in sensor research has been into the area of sensor systems [2]. Accordingly, further scaling of sensor systems, is mandatory for all applications where ultra-miniature size enables the integration of MEMS and other highly integrated systems.

As a magnetic field sensor, GMR sensor offers several key advantages (e.g. high sensitivity, miniature size, contactless install and wear-free work) over other kinds of sensors [3,4]. However, magnetic field sensor systems for demanding applications inevitably contain ferromagnetic parts [5]. These ferromagnetic components are currently used as a part of the sensor itself, like in GMR sensor. The structure of such sensor systems is rather complex, rendering difficult their integration: in the case of GMR sensors, the issues include the mounting of the ferromagnetic component in limited assembly space, and the working distance between ferromagnetic component and GMR sensor chip surface, which is usually 1.5 mm or more [6–8]. Note that if the working distance is smaller, the magnetic intensity generated by the ferromagnetic component is usually so strong that it can upset its pinned layer, thus permanently damaging the sensor element. Furthermore, the GMR sensor bridge in fact converts any field direction to two component signals, independent of their source

* Corresponding author. Address: State Key Laboratory of Robotics and System (HIT), Harbin, PR China. Tel.: +86 451 864 120 42; fax: +86 451 864 183 06.
E-mail addresses: lantianhit@163.com (T. Lan), Hong.liu@dlr.de (H. Liu).

0263-2241/$ - see front matter © 2009 Elsevier Ltd. All rights reserved.
doi:10.1016/j.measurement.2009.03.002

[9]. When a second magnetic field is add to the primary field, the resulting field is a superposed sum of both fields and it may lead to severe disorientation of the angular measurement. These two constraints obstruct the application of GMR sensor in highly integrated field.

In this study, the ultra-miniature GMR sensor system with only 0.5 mm working distance is developed, and the disorientation by other magnetic field is avoided and compensated also based on 3D static magnetic analysis technique. This paper firstly introduces the concept of GMR sensor and finite element modeling. Secondly, the shape and size of ferromagnetic component are compared and optimized by using the 3D static magnetic analysis results. Then a simplified signal processing circuit is also given. Finally the experimental results obtained with the developed method are compared with theoretical results.

2. GMR sensor concept

Giant magneto resistance means the very large change in resistance in ultra-thin magnetic multilayer films. The basic GMR material construction includes a pinned layer and a free layer; the free layer can be influenced by an external magnetic field. An applied magnetic field of adequate magnitude, in the range greater than the saturation field for the free layer and smaller than the standoff field for the pinned layer, will force the free layer magnetization to follow the field when it rotates. With a fixed reference layer magnetization, and an in-step following of the free layer magnetization, magneto resistance is a simple cosine function of the angle of the rotor relative to the stationary sensor. And the resistance R of a spin valve is related to the angle θ between the free and the pinned layer magnetizations in the following equation

$$R/Rp = 1 + 1/2GMR(1 - \cos\theta) \quad (1)$$

where the Rp is the lowest resistance when the two magnetizations are parallel, and the GMR is the maximum percentage magneto resistance.

The angle sensor is used in combination with a planar permanent magnet attached to a live shaft (rotor), as shown in Fig. 1. The permanent magnet is magnetized in-plan thus creating a field that is in the plane of the sensor chip and rotating with the shaft. This field forces the free layer magnetization to rotate in phase with it and the rotor. Therefore the output signal is a sinusoidal function of the angle. With the permanent magnet, sensor design, and their axial configuration the same, the distance between the magnet and the sensor, or working distance, determines the magnitude and distribution of the magnetic field acting on the free layer of the SV resistors. The basic requirement for the working distance is that the lowest field acting on the free layer is large enough to saturate it, and the highest field does not distort the reference layer [7].

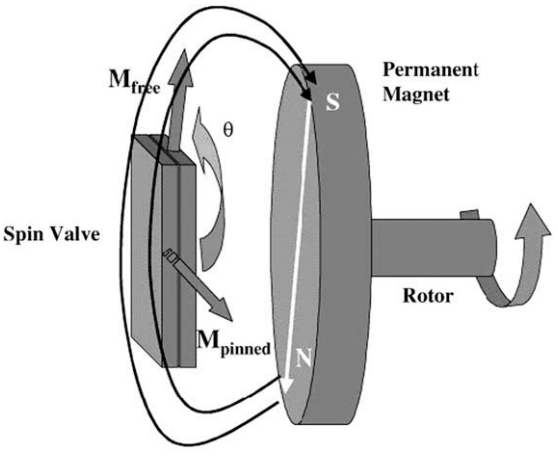

Fig. 1. Schematic of an angle sensor-permanent magnet rotor [7].

3. Finite element modeling (FEM)

The method of finite element modeling is based on a discretization of the solution domain into small regions. The program uses Maxwell's equations as the basis for electromagnetic field analysis. In magneto static problems, the unknown quantity (degree of freedom) is usually the magnetic vector potential, and is approximated by means of polynomial shape functions. Other magnetic field quantities such as magnetic field flux density, magnetic intensity, current density, energy, forces, loss, inductance, and capacitance are derived from the degree of freedom [10]. The size of elements must be small enough to provide sufficient accuracy [11]. In this way, the differential equations of the continuous problem can be transformed into a system of algebraic equations for the discrete problem. The practical problems necessitate usually several thousands of unknowns. However, appropriate numerical techniques have been developed, enabling to obtain the solution of such systems within reasonable time, even when personal computers are used.

As a highly integrated electromechanical system, robot hand needs to complete complex tasks, like fine manipulation, it is often necessary to get enough accurate angular signals to implement some control strategy [12]. Therefore angular sensor plays as a very important role in the sensor system and its signal accuracy affects control effect directly. With high sensitivity and miniature size, GMR sensor is very appropriate for highly integrated system, like DLR/HIT II 5-finger dexterous robot hand.

As above stated, in spite of the benefits which GMR sensor has, there are still some imperfections in highly integrated application. Because in highly integrated system, it does not have enough space to install the sensor and permanent magnet, then the sensor system should be designed to make the best use of the limited space. For example, in the DLR/HIT II dexterous robot hand, the distance between shaft end and GMR sensor chip surface is only 0.5 mm (as shown in Fig. 2). By the limitation of machine structure, there are two types of permanent magnet can be embedded into the shaft end. One is cylinder, the other is cube. In order to ensure enough strength and avoid interference, the diameter of the cylinder permanent magnet should be less than or equal to 2.5 mm, the length of the cube permanent magnet should be less than or equal to 6 mm, and both the thickness should be less than or equal to 1 mm. Face the problems of the limited space

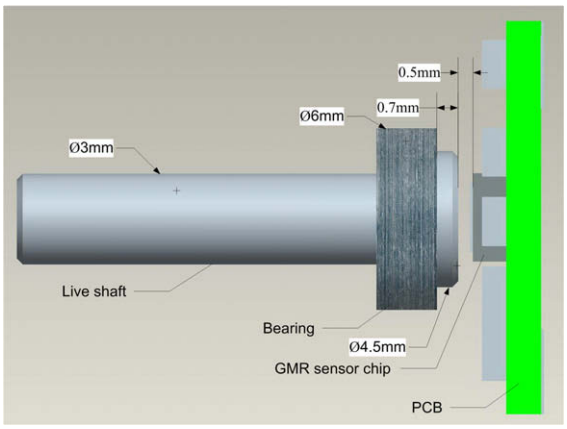

Fig. 2. Application of the GMR sensor in 5-finger dexterous robot hand.

and the demand of precise angular signals, and consider cost and time of sensor development, it is unaccepted that first manufacture permanent magnet and then measure it by measuring apparatus. Therefore, we present a valid method that uses 3D static magnetic analysis technique for designing the type of the permanent magnet to guarantee appropriate direction and magnitude of the magnetic field.

In order to reject disturbance of magnetic field, the live shaft is made of non-magnetic stainless steel material. Then the model can be simplified and only the permanent magnet is analyzed, so the burden of analysis calculation is lightened greatly. The permanent magnets analyzed in this paper are made of NdFeB35 material and have remanence equal to 1.2340 T and coercive force equal to 11339 A/m. The 3D finite element analysis model of a cylinder permanent magnet and a cube permanent magnet are built respectively, and their spatial magnetization vector distributions are also shown. Fig. 3(a) shows a spatial magnetization vector distributions generated by a cylinder permanent magnet ($\Phi 2.5 \times 1$ mm), and Fig. 3(b) represents a spatial magnetization vector distributions generated by a cube permanent magnet ($6 \times 2 \times 1$ mm). From the figure, it can be seen that the magnetization vectors generated by the cube permanent magnet are more planar than those of the cylinder permanent magnet. It is because the length of the cube permanent magnet is bigger than the cylinder permanent magnet. Whereas GMR sensor chip is only sensitive in the parallel plane of the chip, rather than orthogonally to the chip, so the cube permanent magnet is better than the cylinder permanent magnet for application of GMR sensor in this paper.

However, GMR materials not only require the direction of magnetization vector, but also need the magnitude of magnetic intensity in its working range to avoid the sensor element damage and signal distortion. Therefore the distribution of the magnetic intensity in the limited space is must be achieved. Fortunately, 3D static magnetic analysis technology can make these problems easy to be solved. With the help of 3D FEM software, we acquire 3D magnetic field distribution of different permanent magnet type (Figs. 4 and 5). From the date sheet of GMR sensor chip, we know the working range absolute values are from 2388 A/m to 15,920 A/m, namely B and C in Figs. 4 and 5. It means that the GMR sensor chip must be in domain between B and C. Fig. 4 shows a spatial distribution of magnetic intensity magnitude (capped plane along $X = 0$ mm and $Z = 1$ mm) generated by a cube permanent magnet which size is

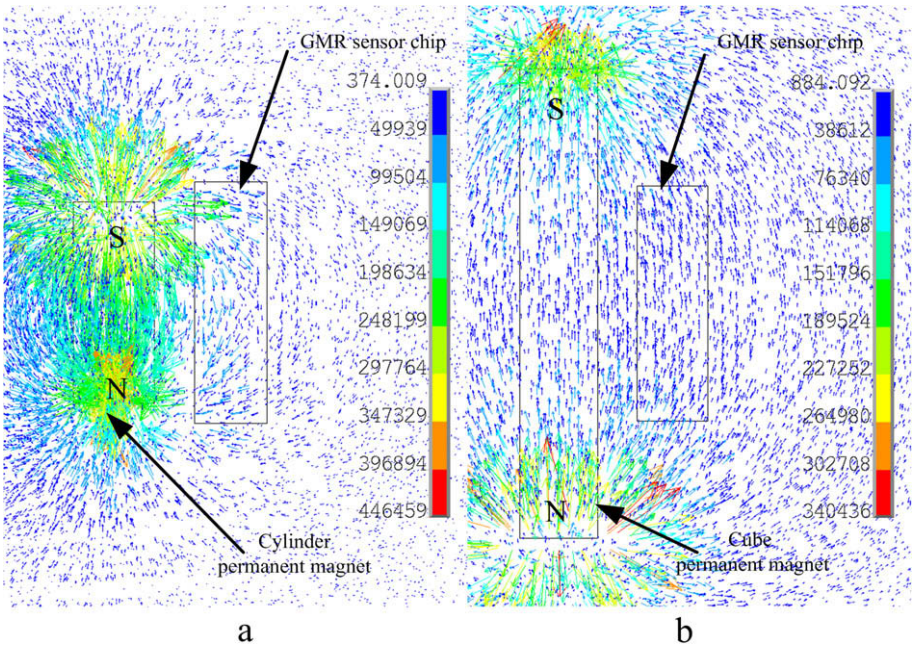

Fig. 3. A spatial magnetization vector distributions generated by (a) cylinder permanent magnet ($\Phi 2.5 \times 1$ mm), (b) cube permanent magnet ($6 \times 2 \times 1$ mm).

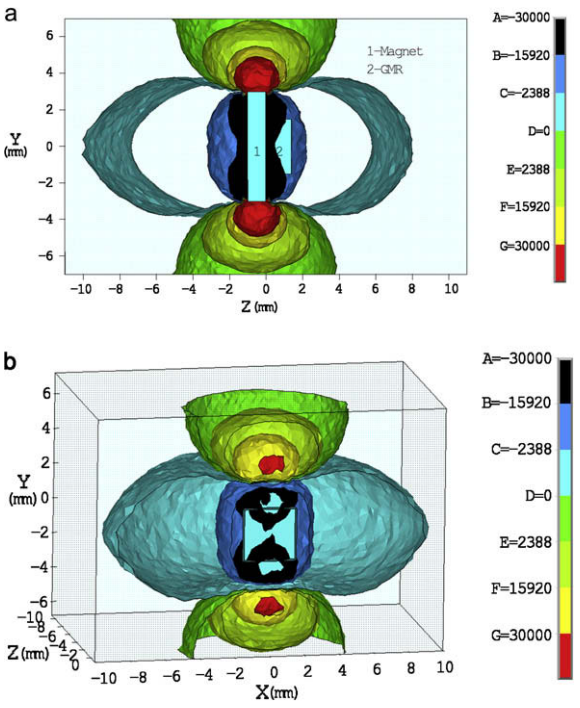

Fig. 4. A spatial distribution of magnetic intensity magnitude generated by a cube permanent magnet which size is $6 \times 2 \times 1$ mm. (a) Capped plane along $X = 0$ mm, (b) capped plane along $Z = 1$ mm.

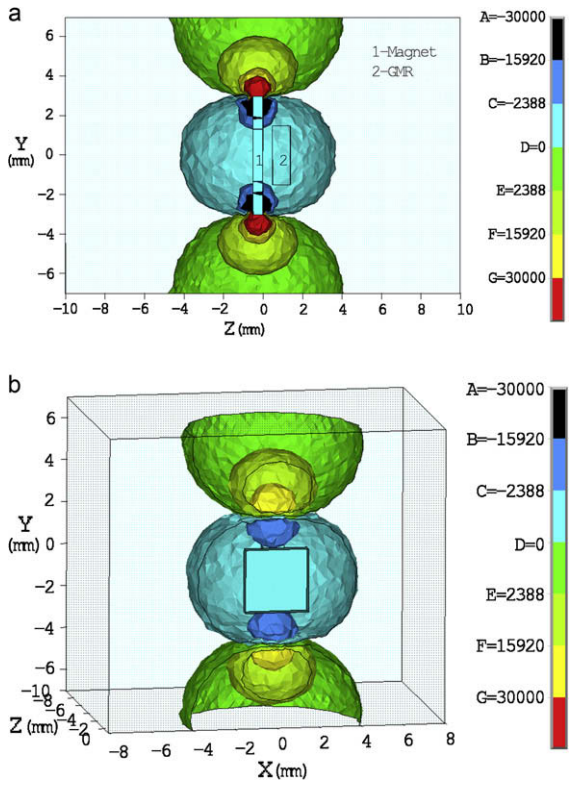

Fig. 5. A spatial distribution of magnetic intensity magnitude generated by a cube permanent magnet which size is $6 \times 1 \times 0.5$ mm. (a) Capped plane along $X = 0$ mm, (b) capped plane along $Z = 1$ mm.

$6 \times 2 \times 1$ mm. From the figure, it can be seen that most of the GMR sensor chip are in domain between A and B that exceed the working range. Therefore the GMR sensor chip is unable to work normally, and we must find a way to make the GMR sensor chip in its working range, i.e. in the domain between B and C.

It is well known that the magnitude of magnetic intensity can be diminished by dwindling the width and thickness of permanent magnet. Based on the 3D static magnetic analysis technique, the size can be dwindled step by step to achieve the adequate magnitude of magnetic intensity rather than first manufacture different sizes of permanent magnets and then measure them. Finally, the right size of the permanent magnet is acquired (as shown in Fig. 5). From the figure, it can be seen that the whole body of the GMR sensor chip is in domain between B and C. Therefore the size ($6 \times 1 \times 0.5$ mm) is the right one that can generate adequate magnitude of magnetic intensity. Additionally, the simulation results can be used to put other permanent magnet outside the working domain to avoid disorientation. And it also can be used to compensate deviation in the succeeding digital processing.

4. Signal detection and processing

The best way to get a high signal-gain for sensing the GMR resistance change is to build up a Wheatstone bridge and sensing the differential voltage. In this case two opposite reference layer magnetizations are necessary to get the highest resistance change (Fig. 6). One bridge can measure a 180° angle-range, so it is necessary to build up two orthogonal bridges to detect angles of 0°–360°. In this case, we need four different reference magnetization directions in total, which define the measurement angle-orientation and turning direction regarding to the chip package.

The percent change of resistance available with this GMR material is about 5%. It means that the amplitude of output signal is too small to content with the demands of high accuracy angle detection. So a pair of analog multipliers and four low pass filters of the signal detection circuit are used to extract the amplitude of the signal and its phase. The advantages of this configuration are simplicity, low component count, low cost, and ultra-miniature size.

Take sine signal for example, the first low pass filter has a capacitor in parallel with the feedback resistor, so the circuit has a 6 dB per octave roll-off after a closed-loop 3 dB point defined by $Fc = 1/(2 \cdot \pi \cdot R2 \cdot C1)$. And output voltage below this corner frequency is defined by Eq. (2). The circuit may be considered as an AC integrator at frequencies well above Fc. However, the time domain response is that of a single RC rather than an integral. Parallel combination of $R3$ and $R4$ should be chosen equal to parallel combination of the $R1$ and $R2$ to minimize errors due to bias current. The amplifier should be compensated for unity-gain or an internally compensated amplifier can be used.

$$V_{\sin\_out} = \frac{R1 + R2}{R3 + R4} \cdot \frac{R4}{R1} \cdot 3.3 - \frac{R2}{R1} \cdot V_{\sin\_in} \tag{2}$$

The second filter is a low pass filter formed by $R5$ and $C2$, which pretends minimizing the bandwidth of noise and limiting the valid spectrum in the system. Therefore the

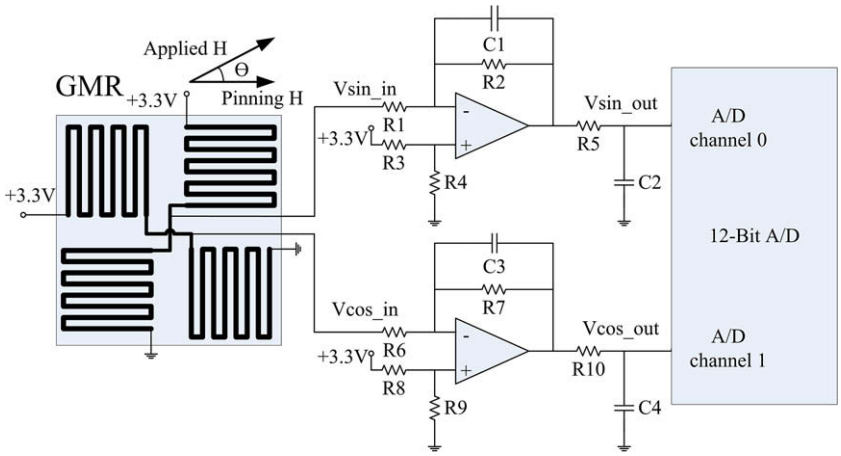

Fig. 6. Schematic diagram of the GMR sensors signal detection and processing.

cut-off frequency for this filter is determined by the pole $Frc = 1/(2 \cdot \pi \cdot R5 \cdot C2)$.

5. Experimental results

The ultra-miniature GMR sensor system has been developed using the above explained method, which fulfills the requirements of angular measurement and integrated level for DLR/HIT II 5-finger dexterous robot hand (as shown in Fig. 7).

Experiments have been carried out to verify the validity of the model. When a constant voltage is applied to the bridge (as shown in Fig. 6), the output voltage $V_{\text{sin\_in}}$ is a sine function, and $V_{\text{cos\_in}}$ is a cosine function of the angle between GMR sensor chip and the live shaft, with a common direct current offset half of the supply voltage +3.3 V. The output signals are captured by a microcontroller and plotted with a 0.5 mm working distance, along with the theoretical sine and theoretical cosine curves (as shown in Fig. 8). The errors between measured values and theoretical values are also shown in Fig. 9. The curve with circles represents sine error and the curve with squares is cosine error.

The angle is extracted from the measured sine and measured cosine function, with the four quadrant inverse tangent function of these two values. The angle is obtained without discontinuity or dead angle over full 360° (as shown in Fig. 10).

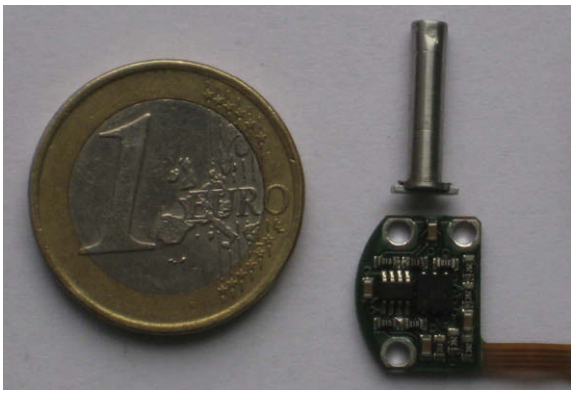

Fig. 7. GMR sensor system of DLR/HIT II 5-finger dexterous robot hand.

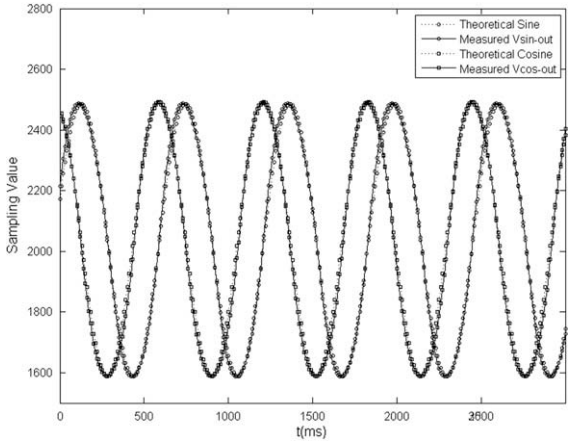

Fig. 8. Output signals of the GMR sensor compared with theoretical sine and cosine curves.

Absolute non-linearity is defined as the deviation from the best linear fit with a unitary slope. ANL is often chosen because of the 360° periodicity. The measurement result for a 360° rotation magnetic field showed that the ANL error is ±6° without any residual offset compensation. As shown in Fig. 10, an ANL of second harmonic is observed (dashed curve), and the sources of this type of ANL are gain mismatch and non-orthogonality of the sensor axes. It can be seen that the ANL repeat periodically. Therefore one cycle of the offset errors can be use to compensate the measured signals. After offset compensation, the angular error (solid curve) is less than ±1°, which fulfills the requirements of angular measurement in DLR/HIT II 5-finger dexterous robot hand and many other applications.

6. Conclusions

Based on 3D static magnetic analysis technique, the ultra-miniature GMR sensor system with only 0.5 mm

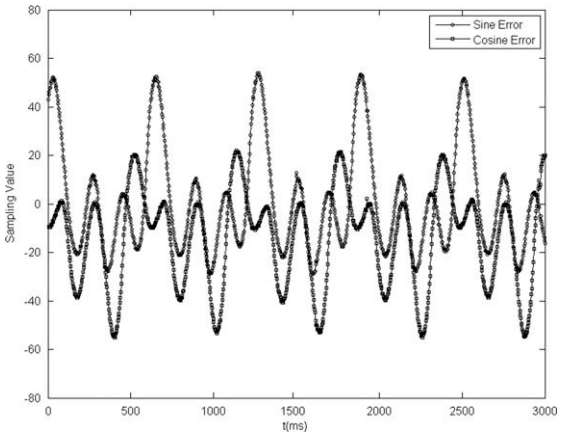

Fig. 9. The errors between measured values and theoretical values.

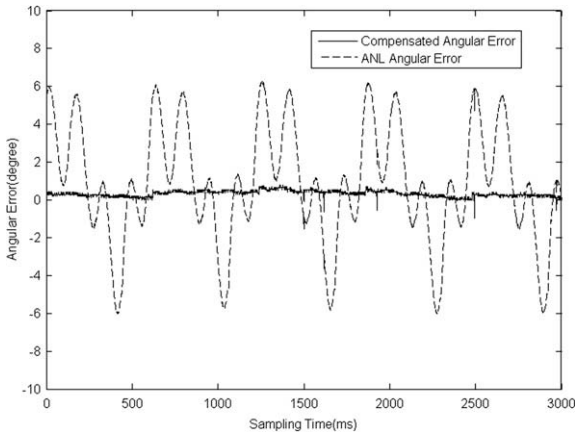

Fig. 10. The angular errors of ANL and compensation obtained using the four quadrant inverse tangent function.

working distance is newly developed for highly integrated DLR/HIT II 5-finger dexterous robot hand. Through the experiment results mentioned above, the output characteristics of the GMR sensor system have been obtained such as the measurement range, accuracy, working distance and the repeatability. It also has the qualities of ultra-miniature size, simple structure and high reliability, all of which makes up for the shortcomings of traditional measurement sensors, such as bulk, complexity, high cost, strict demand to working environment and assembly difficulty. This work also has established a good base for further study of magnetic sensor for micro sensor systems of MEMS and highly integrated systems.

Acknowledgements

This project is supported by the National High Technology Research and Development Program of China (863 Program) (No. 2006AA04Z255) and Self-Planned Task (NO. SKLR200801A01) of State Key Laboratory of Robotics and System (HIT).

References

[1] C. Hierold, C. Stampfer, T. Helbling, et al., CNT based nano electro mechanical systems (NEMS), in: Proceedings of the IEEE 2005 International Symposium on Micro-NanoMechatronics and Human Science, Nagoya, Japan, 8–9 November, 2005, pp. 1–4.
[2] R.S. Popovic, J.A. Flanagan, Sensor microsystems, in: Proceedings of 20th International Conference on Microelectronics, Nis, Septemper 12–14, 1995, pp. 531–537.
[3] C.P.O. Treutler, Magnetic sensors for automotive applications, Sensors and Actuators A 91 (2001) 2–6.
[4] C. Giebler, D.J. Adelerhof, A.E.T. Kuiper, et al., Robust GMR sensors for angle detection and rotation speed sensing, Sensors and Actuators A 91 (2001) 16–20.
[5] Radivoje S. Popovic, Predrag M. Drljaca, Pavel Kejik, CMOS magnetic sensors with integrated ferromagnetic parts, Sensors and Actuators A 129 (2006) 94–99.
[6] G. Malinowski, M. Hehn, F. Montaigne, et al., Angular magnetic field sensor for automotive applications based on magnetic tunnel junctions using a current loop layout configuration, Sensors Actuators A (2008), doi:10.1016/j.sna.2008.02.009.
[7] D.X. Wang, J. Brown, T. Hazelton, et al., 360° angle sensor using spin valve materials with SAF structure, IEEE Transactions on Magnetics 41 (10) (2005) 3700–3702.
[8] NVE Corporation, Datasheet of the magnetic sensor AAV001-11 from NVE Corporation. <http://www.nve.com/Downloads/catalog.pdf>, 2008 (cited 25.09.08).
[9] W. Granig, C. Kolle, D. Hammerschmidt, et al., Integrated gigant magnetic resistance based angle sensor, in: IEEE Sensors 2006, EXCO, Daegu, Korea, October 22–25, 2006, pp. 542–545.
[10] T. Kefalas, G. Kalokiris, A. Kladas, et al., Design of skewed mounted permanent magnet synchronous generators based on 2D and 3D finite element techniques, Journal of Materials Processing Technology 161 (2005) 288–293.
[11] T. Nakata, N. Takahashi, K. Yoneda, Numerical analysis of flux distribution in permanent magnet stepping motors, IEEE Transactions on Magnetics 14 (1978) 548–550.
[12] H. Liu, P. Meusel, N. Seitz, et al., The modular multisensory DLR-HIT-Hand, Mechanism and Machine Theory 42 (2007) 612–625.